Multilevel blazed gratings in resonance domain: an alternative to the classical fabrication approach

M. Oliva,[1,*] T. Harzendorf,[1] D. Michaelis,[1] U. D. Zeitner,[1] and A. Tünnermann[1,2]

[1] *Fraunhofer Institute for Applied Optics and Precision Engineering, Albert-Einstein-Strasse 7, 07745 Jena, Germany*
[2] *Institut für Angewandte Physik, Friedrich-Schiller-Universität Jena, Max Wien Platz 1, 07743 Jena, Germany*
**maria.oliva@iof.fraunhofer.de*

Abstract: In this paper we present a novel technological approach for the fabrication of multilevel gratings in the resonance domain. A coded chromium mask is used to avoid alignment errors in electron beam lithography, which typically occur within the standard multistep binary micro-optics technology. The lateral features of all phase levels of the grating are encoded in a single chromium mask. The final profile of the structure is obtained by selective etching process for each level. This new technological method is applied for the fabrication of two different three-level gratings in resonance domain. The corresponding optical response as well as structural characterizations are presented and discussed. In particular, a first order diffraction efficiency of 90% is demonstrated for a grating period twice the wavelength at normal incidence.

OCIS codes: (050.1950) Diffraction gratings; (050.5745) Resonance domain; (220.3740) Lithography; (220.4241) Nanostructure fabrication.

References and links

1. M. B. Fleming and M. C. Hutley, "Blazed diffractive optics," Appl. Opt. **36**(20), 4635–4643 (1997).
2. G. J. Swanson, "Binary optics technology: theoretical limits on the diffraction efficiency of multilevel diffractive elements," MIT Tech. rep. 914 (MIT, 1989).
3. O. Sandfuchs, R. Brunner, D. Pätz, S. Sinzinger, and J. Ruoff, "Rigorous analysis of shadowing effects in blazed transmission gratings," Opt. Lett. **31**(24), 3638–3640 (2006).
4. S. Astilean, P. Lalanne, P. Chavel, E. Cambril, and H. Launois, "High-efficiency subwavelength diffractive element patterned in a high-refractive-index material for 633 nm," Opt. Lett. **23**(7), 552–554 (1998).
5. P. Lalanne, "Waveguiding in blazed-binary diffractive elements," J. Opt. Soc. Am. A **16**(10), 2517 (1999).
6. M.-S. L. Lee, P. Lalanne, J.-C. Rodier, and E. Cambril, "Wide-field-angle behavior of blazed-binary gratings in the resonance domain," Opt. Lett. **25**(23), 1690–1692 (2000).
7. H. J. Hyvärinen, P. Karvinen, and J. Turunen, "Polarization insensitive resonance-domain blazed binary gratings," Opt. Express **18**(13), 13444–13450 (2010).
8. H. Iizuka, N. Engheta, H. Fujikawa, K. Sato, and Y. Takeda, "Role of propagating modes in a double-groove grating with a +1st-order diffraction angle larger than the substrate-air critical angle," Opt. Lett. **35**(23), 3973–3975 (2010).
9. E. Noponen, J. Turunen, and A. Vasara, "Parametric optimization of multilevel diffractive optical elements by electromagnetic theory," Appl. Opt. **31**(28), 5910–5912 (1992).
10. M. Oliva, D. Michaelis, T. Benkenstein, J. Dunkel, T. Harzendorf, A. Matthes, and U. D. Zeitner, "Highly efficient three-level blazed grating in the resonance domain," Opt. Lett. **35**(16), 2774–2776 (2010).
11. M. B. Stern, "Binary optics fabrication," in *Microoptics: Elements, Systems and Application*, H. P. Herzig, ed. (Taylor & Francis, 1997), pp. 53–85.
12. U. D. Zeitner and E. B. Kley, "Advanced lithography for micro-optics," Proc. SPIE **6290**, 629009 (2006).
13. C. David, "Fabrication of stair-case profiles with high aspect ratios for blazed diffractive optical elements," Microelectron. Eng. **53**(1-4), 677–680 (2000).
14. M. Kuittinen and J. Turunen, "Mask misalignment in photolithographic fabrication of resonance-domain diffractive elements," Opt. Commun. **142**(1-3), 14–18 (1997).
15. U. D. Zeitner, D. Michaelis, E.-B. Kley, and M. Erdmann, "High performance gratings for space applications," Proc. SPIE **7716**, 77161K (2010).
16. M. Oliva, T. Benkenstein, J. Dunkel, T. Harzendorf, A. Matthes, D. Michaelis, and U. D. Zeitner, "Smart technology for blazed multilevel gratings in resonance domain," Proc. SPIE **7716**, 77161L (2010).

#148535 - $15.00 USD Received 2 Jun 2011; revised 8 Jul 2011; accepted 8 Jul 2011; published 15 Jul 2011

1. Introduction

Multilevel diffraction gratings are a well-known family of diffractive elements that can accomplish the blazing optical function; i.e. the incoming light can be highly efficient redirected in one diffraction order. Usually, the profile of a multilevel blazed grating is the stepwise approximation of a classical linear blazed grating, with the typical triangular sawtooth shape [1]. In the resonance domain, where the period is close to the operating wavelength, this approximation leads to a drop in the efficiency due to the shadowing effect [2,3]. In order to minimize the shadowing effect the binary blazed gratings have been proposed. Such type of gratings are diffractive elements made of different features size subwavelenght structures arranged along the grating period [4–7], in order to tailor the effective refraction index on the basis of the effective medium theory. In some aspects this solution is less complicated, because a traditional binary optics technology is needed only. However, the required aspect ratio, i.e. the ratio of depth to lateral feature size, is typically considerably larger than 5. Thus, this approach becomes not more suitable when the illumination wavelength is so short that the minimum feature size of the subwavelength structures is below the technological capabilities. Additionally, due to their intrinsic symmetry, the binary blazed gratings achieve their maximum efficiency in the Littrow configuration. It is not simple to shift the maximum efficiency to arbitrary incidence angles [8], for example to normal incidence. For applications where such kind of gratings is needed, the approximation of the blazed profile by a multilevel blazed grating remains the most appropriate solution. To reach the highest possible efficiencies, the blazed profile is not obtained by a simple approximation of the linear continuous profile as one might conclude from the scalar theory. The most favorable grating structures can be designed by a parametric optimization of each level, as suggested by Noponen at al [9].

In this paper, we present a new technological approach for the fabrication of such multilevel blazed gratings in the resonance domain. The aim to develop a new technology concerns the need to avoid the alignment and sizing errors that occur in the standard multistep binary optics technology. These errors are not negligible in the resonance domain, because related structural artifacts become comparable with the multilevel feature sizes. Consequently, the diffraction efficiency of the gratings can be seriously affected. The basic idea of this new technology, which we called *relaxed alignment technology*, consists in the use of a single etching mask for the whole fabrication process. This leads to the necessity to codify the lateral features sizes of each grating level during the first step of the lithographic process.

To test and evaluate the new technological approach, two multilevel blazed gratings, working in two different regions of the resonance domain have been fabricated and characterized. The achieved results are presented and discussed in this paper.

2. Three-level gratings design

In this paper we focus on multilevel gratings in the resonance domain, i.e. the grating period is only a few times larger than the wavelength of the light the grating is used with. By optimizing the grating for high diffraction efficiency in the 1st diffraction order one obtains a non-linear profile within one period. As a consequence the levels do not have the same depth and linear increasing width as it would be the case for a standard sawtooth like profile. For very small period-wavelength-ratios even a three-level grating as the most simple multi-level element shows a remarkably high efficiency at least for one light polarization [9]. A physical interpretation for the high efficiency of those three-level gratings, based on three beams interference mechanism, has been suggested recently [10]. But even for larger period to wavelength ratios three-level elements are of great interest because of their minimally required technological effort.

Figure 1 shows the design parameters as well as the relevant diffraction efficiencies of two different three-level gratings. The gratings differ in illumination wavelength, application and required specifications.

#148535 - $15.00 USD Received 2 Jun 2011; revised 8 Jul 2011; accepted 8 Jul 2011; published 15 Jul 2011

(a)

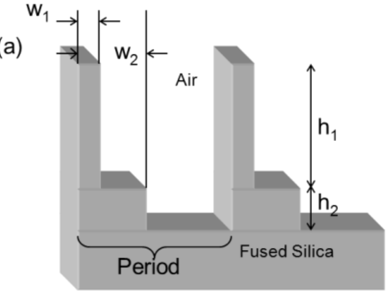

(b)

Grating	A	B
Period	1.866 µm	1.266 µm
Lambda	416 nm	633 nm
Refractive index	1.46847	1.45701
w_1	519 nm	200 nm
w_2	1.202 µm	580 nm
h_1	333 nm	778 nm
h_2	281 nm	394 nm

(c) (d)

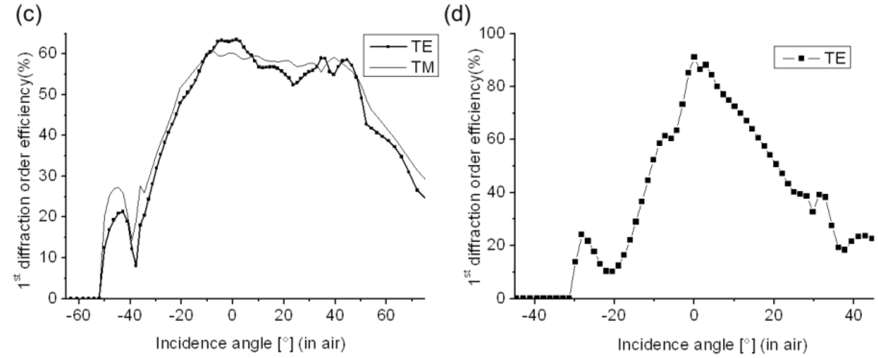

Fig. 1. (a) Schematic representation of a three-level grating profile. (b) Table with the parameters of grating A and B considered in this paper. (c) and (d) Efficiency of the first diffraction order versus the angle of incidence in air for grating A and B, respectively

Usually, the specifications depend very strongly on the type of application.

The first three-level grating, here indicated as grating A, is the result of a preliminary design of a spectrometer grating for astronomical measurement, which is a typical high-end application. This means that the high diffraction efficiency of a single diffraction order is not always the grating parameter of highest importance. Especially in optical systems in which the grating is part of an imaging arrangement, like in a spectrometer, the resulting overall performance and spectral resolution is also dependent on parameters like the wavefront-error, the stray-light level, and the polarization sensitivity of the grating.

The illuminating wavelength of grating A is 416 nm and the period is p = 1.877 µm. It is designed to work close to normal incidence and to be polarization invariant; the efficiency is rather constant for a large range of illuminating incidence angles. The design is quite close to the scalar approximation for a standard blazed grating operating in the same conditions. For this reason the efficiency of the optimized grating (ca.62%) is not very much higher than that one of the classical multilevel element (ca. 55%).

The second grating (grating B) is a highly efficient and highly dispersive blazed grating operating at an illumination wavelength of 633 nm for TE polarization. It is a transmission grating for the first diffraction order with an optimal efficiency of about 90% at normal incidence. The period p = 1.266 µm is two times the wavelength. Therefore, the grating is working in really deep resonance domain.

The two gratings are illuminated through the substrate and the first diffraction order is transmitted in air. The parameters of the two gratings are defined in the table of Fig. 1b.

Both gratings operate in resonance domain, but in two different regions. Consequently, they differ in the profile’s shape. Because of the smaller period and the large depth of the upper level (778 nm) grating B is the most critical one from a technological point of view.

#148535 - $15.00 USD Received 2 Jun 2011; revised 8 Jul 2011; accepted 8 Jul 2011; published 15 Jul 2011

3. Limit of standard technology: multistep binary optics technology

The standard technology for the fabrication of blazed multilevel gratings consists of a multistep binary optics approach [11]. For a three or four-level grating two consecutive lithography steps are needed which are schematically illustrated in Fig. 2a. In the initial step of the fabrication process, a substrate (e.g. fused silica) is covered first with chromium followed by an electron-beam resist layer (Fig. 2a (i)). The resist is exposed by electron beam lithography to achieve the first desired profile width (w_2). The developed resist pattern is subsequently transferred by reactive ion etching (RIE) into the chromium layer (Fig. 2a (ii)) which henceforth acts as a hard mask for RIE etching (height h_2) of the binary structure into the fused silica substrate [12] (Fig. 2a (iii)-(iv)). Then the same process is repeated to realize the second binary grating profile with the width w_1 and the height h_1 on top of the first binary structure (Fig. 2a (v)-(ix)).

There are two main problems related to this technology. The first issue is due to the alignment errors that could occur between the two lithographic exposures of the different levels. This misalignment between the first etched level and the resist pattern leads to artifacts in the final grating profile (see Fig. 3a)).

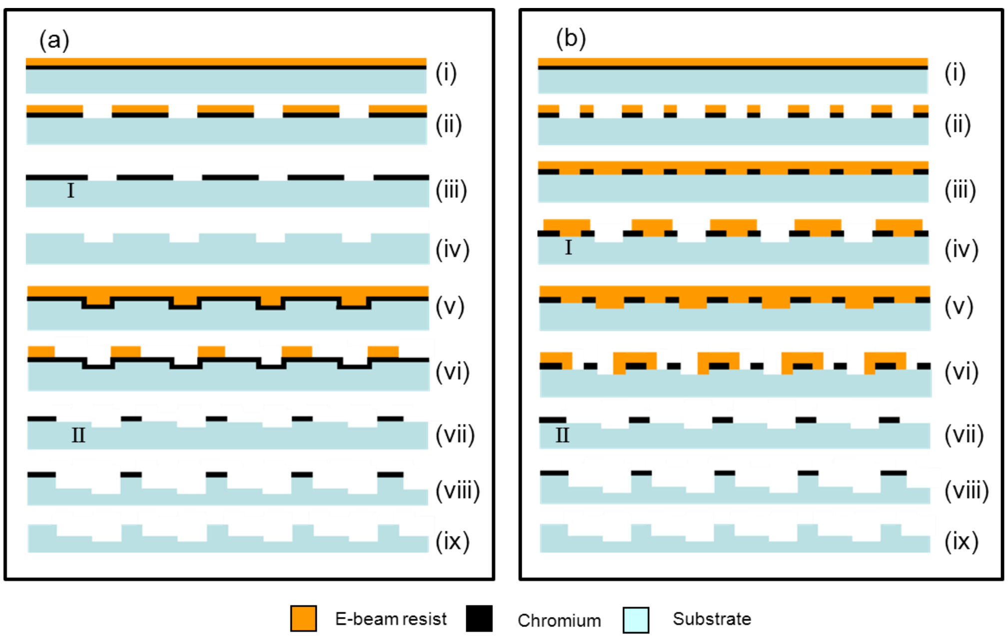

Fig. 2. Sequence of the most relevant steps of the fabrication process for a three-level grating. (a) Standard technology approach (b) *Relaxed Alignment Technology* approach. In step “I” and “II” equivalent masks for the two approaches are used for the deep etching into the substrate of level 1 and 2, respectively.

The other problem is related to the non-uniformity of the chromium and resist layers of the second fabrication step. As a consequence, the profile of the upper binary grating might be not well defined and its dimensions could change over the grating area generating a kind of sizing error. Sizing and alignment errors could happen simultaneously as schematically illustrated in Fig. 3b.

One technological solution to avoid this problem related to the non-uniform chromium and resist layers has been suggested by David [13]. This approach is based on the use of a really thin resist layer (50-80 nm) and stepwise etching through two different metal masks (Cr and Al).

Another solution consists in the use of an additional resist layer coated on the top of the first etched binary grating which acts like a planarization level for the second chromium and

#148535 - $15.00 USD Received 2 Jun 2011; revised 8 Jul 2011; accepted 8 Jul 2011; published 15 Jul 2011

resist layer deposition. This approach has been recently adapted to the fabrication of a three-level grating [10].

However, these approaches, the two-metal masks [13] and the three-resist layer technology [10], do not solve the problems related to misalignments between sequential lithography exposures.

In resonance domain both technological problems may have a major impact on the grating performance, because such imperfections are not negligible [14] with respect to the small feature sizes of the diffractive elements. Figure 3 shows the influence of simultaneously occurring sizing and alignment errors on the phase and the diffraction efficiency for the gratings reported in this paper. The misalignment between the first etched level and the thereon structured resist pattern could appear in both transverse grating directions (see upper drawings in Fig. 3a). A wrong shift of the second resist structure in the left direction (here called minus direction: m) results in grating profiles which are topological different to that ones occurring for a right direction misalignment (here called plus direction: p). The two types of potentially appearing profiles are illustrated in the lower drawings of Fig. 3a. In addition to these alignment imperfections the profile and the dimension of the upper grating level could be affected by the sizing error. Here we simply model this effect by an increase or a decrease (labeled with + or -) of the upper level (see Fig. 3b). For the simulations sizing errors of +/–20 nm and alignment errors of +/–20 and +/–40 nm are considered which are typical values for multilevel electron-beam-lithography processes. Numerical simulations predict that there are changes of about 10% of the relevant diffraction efficiencies for both gratings (grating A and B) due to these technological difficulties (see left graphs in Figs. 3c, 3d). Because the dimension of the structural errors may change across the grating area variations of the accumulated phase could cause wavefront errors. For the grating A wavefront errors of about 3% in terms of the operation wavelength are predicted. Those wavefront errors would typically increase for decreasing grating periods. In case of grating B a wavefront error of even a tenth of the wavelength would appear.

The limits of standard multistep binary optics technology show that a new technological approach is required for the fabrication of high quality multilevel gratings in resonance domain. Especially, as in nowadays such kind of gratings is moving from research to industrial applications. The dimensions of the grating's area are continuously increasing. The requirements about homogeneity in the topology of the structures and optical performances become higher and have to be fulfilled [15].

#148535 - $15.00 USD Received 2 Jun 2011; revised 8 Jul 2011; accepted 8 Jul 2011; published 15 Jul 2011

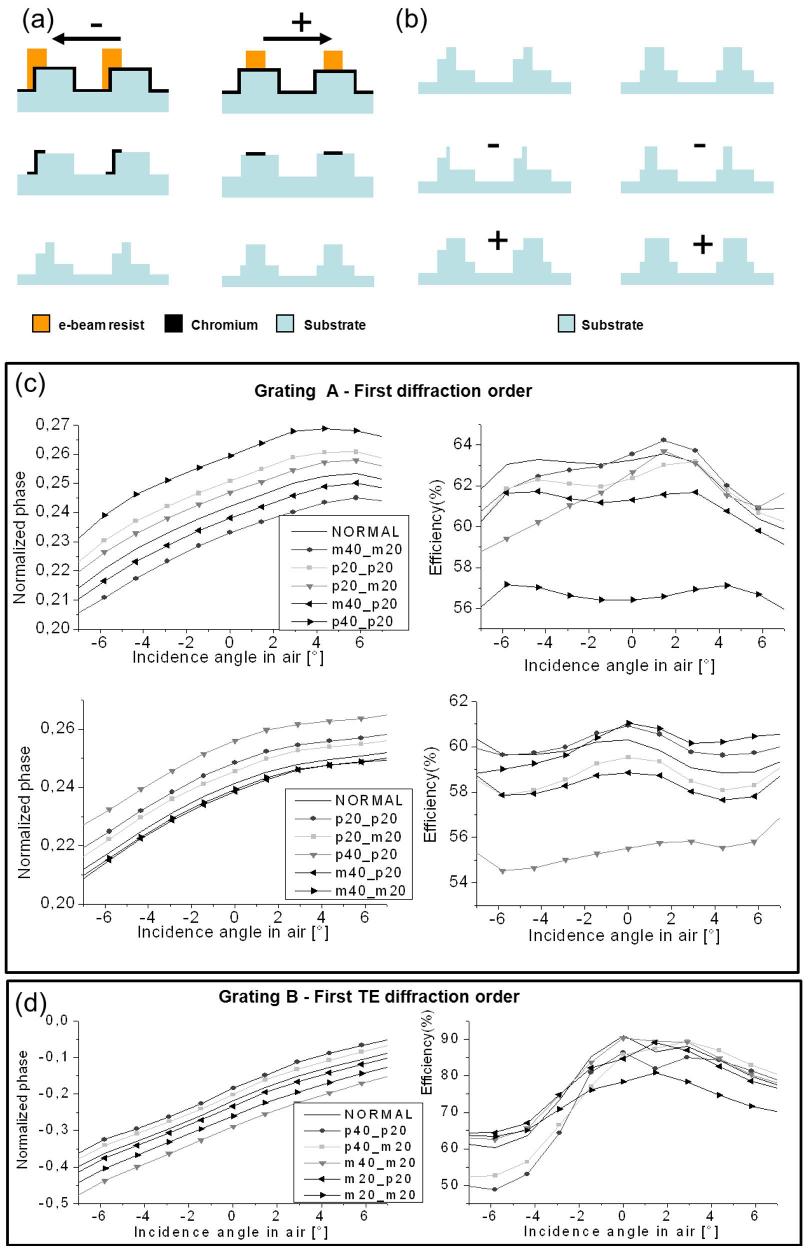

Fig. 3. Influence of sizing and alignment error on the profile and diffraction efficiencies of the three-level gratings reported in this paper. a) Alignment errors: the "minus" sign indicates a shift of the second level resist mask with respect to the already etched level in the left direction, the "plus" sign in the right direction. The resulting structure's profiles are shown at the bottom of the picture. (b) Effect of sizing errors in combination with the alignment errors shown in (a). Here, the "plus" and "minus" signs indicate an increase or decrease of the upper bar's size respectively. (c),(d) Effect of simultaneous alignment and sizing errors on the relevant diffraction efficiencies and corresponding first order phase accumulation of grating A (c) and grating B (d). The phases correspond to a path length normalized to the operating wavelength. In the legend the first and the second numbers (expressed in nanometers) are related to alignment and sizing error, respectively. The "p" and "m" are used as abbreviation of "plus" and "minus" signs.

4. Relaxed alignment technology for multilevel structures

In the standard multilevel technology for a three or four height level structure, the lateral dimensions of each level are coded in two different masks and superimposed by two distinct binary fabrication processes. As discussed above, this may lead to inevitable alignment and sizing errors. A possibility to avoid such kinds of errors would be the encoding of the lateral dimension of all levels in a single mask. This is the basic idea of the *Relaxed Alignment Technology* discussed in the following. In this approach, a single coded chromium mask is used in the whole fabrication process.

A coded chromium mask means that it contains the relevant lateral features of each level, as shown in Fig. 2b. The first lithographic exposure is used for the definition of these features (Fig. 2b (ii)). Then the pattern is transferred into the chromium mask. Like in the standard approach (Fig. 2a), the chromium mask acts as hard mask to transfer the exposed geometries into the substrate (here: fused silica).

For the fabrication of a three-level grating, the etching of two different phase levels is needed. Because all lateral information is coded in the mask, before the deep etching into the substrate, it is needed to cover the part (means the phase level) which should not be transferred during the first deep etching process. A resist mask is suitable for this purpose. Thus, a lithography step is needed to exposure this mask (Fig. 2b (iii, iv)). Now, the phase level which has to be etched is well defined due to the already existing chromium mask. Consequently, the cover resist mask can be exposed with considerably relaxed requirements on the alignment. The needed accuracy in the alignment is relaxed to the minimum feature size of the chromium structures. The pattern is transferred into the fused silica substrate by a RIE (Reactive Ion Etching) process until the height level h_2 is reached (Fig. 2b (iv)).

To proceed further with the fabrication of the three-level grating, we have now to remove the part of the chromium mask that is not needed anymore. An additional lithographic exposure (Fig. 2b (v,vi)) is used to protect the chromium pattern that has to be preserved after the next chromium etching process. Also this step is not challenging with respect to the alignment accuracy. After removing the protecting resist structure (Fig. 2b (vii)) the second level (h_1, w_1) is transferred into the fused silica substrate (Fig. 2b (viii)). The last step of the fabrication process consists in removing the remaining chromium mask (Fig. 2b (ix)), just the same as in the standard technology. Now, the three-level profile is completely transferred into the substrate.

As already mentioned, the *Relaxed Alignment Technology* is a good approach to avoid the alignment errors that typically occur within the standard multistep binary technology. Nevertheless, it has to be taken into account that an additional lithographic exposure is needed. This increases the fabrication effort to realize the grating.

Another aspect of this technology which should be addressed is that the use of a combined resist-chromium mask for the etching of the phase level (h_2, w_2) limits the achievable depth for h_2 (see Fig. 2b (iv)). It originates from the relatively low etching rate selectivity of the resist with respect to the fused silica in the RIE process (typically < 1 to 3). Additionally, the resist thickness should be smaller than a few hundred nanometers in order to obtain the required resolution.

A further limitation of this technology could arise from charging effect of the resist during the successive e-beam lithography steps due to the reduction of the chromium mask area. This charging effect could cause additional misalignments of the patterned structures. The resulting overlay error could have a similar effect than the misalignment error in the standard approach.

Despite of this limitation, the idea to use a resist-chromium mask adds high flexibility to the profile of the structures that can be fabricated.

#148535 - $15.00 USD Received 2 Jun 2011; revised 8 Jul 2011; accepted 8 Jul 2011; published 15 Jul 2011

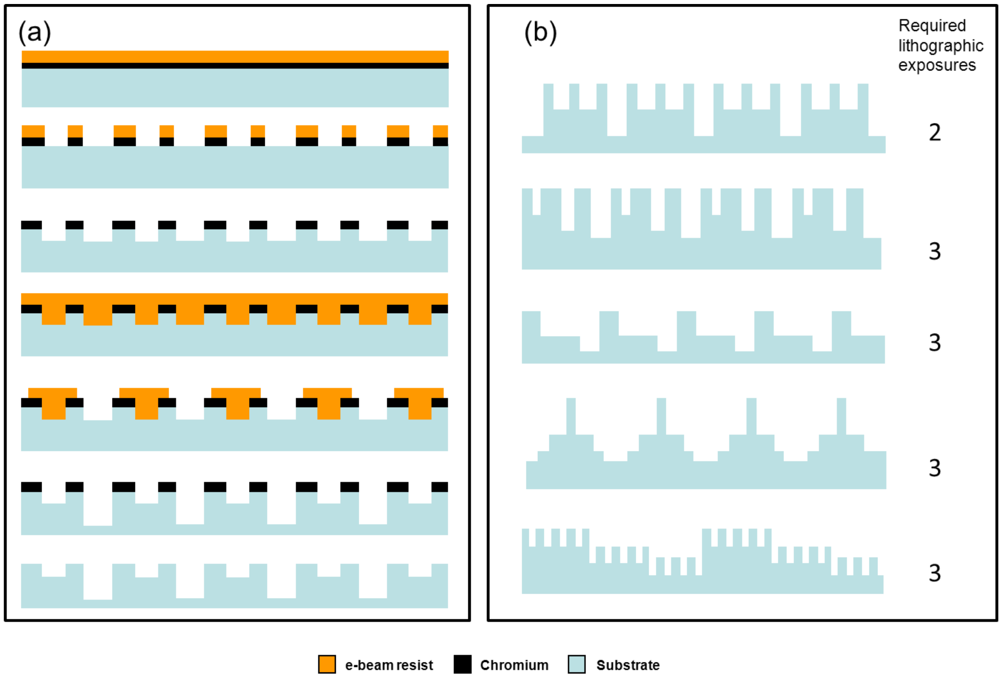

Fig. 4. (a) Sequence of most relevant technological steps for the fabrication of a multilevel structure by *Relaxed Alignment Technology* approach using the same coded chromium mask like in Fig. 2b but leading to a different diffractive structure. (b) Examples of structures that can be realized by this approach.

The Fig. 4a demonstrates that the same initial chromium mask needed for a three-level grating (Fig. 2b (ii)) is suitable to achieve another grating structure where only two lithographic steps are needed. By a smart variation of the sequential exposure and etching steps different structures such as binary and multilevel gratings or a combination of both could be realized. Some examples of such structures are shown in the Fig. 4b; e.g. effective medium, multilevel or multilevel-effective medium gratings. Different design considerations show that such patterns exhibit beneficial optical properties in special gratings applications. However, their discussion is beyond the scope of this paper.

5. Gratings fabrication and characterization

The three-level gratings, described in this paper, have been fabricated on a 6” fused silica mask blank. For each grating design an array of 9 gratings has been realized in order to optimize the exposure and the etching parameters. The mask blank was covered with 80 nm Cr layer and 300 nm layer of e-beam resist FEP 171(Fuji-Film), a chemical amplified e-beam resist. After a pre–exposure bake step, the sample has been exposed with the electron beam system Vistec SB350 OS (Vistec Electron Beam GmbH, Jena). The grating pattern was written at a 15 mm x 15 mm area enabling a convenient optical characterization. The exposure process to write a single grating lasted less than 20 minutes for each lithographic step. Two kinds of alignment marks have been used, in particular a first mark for the global alignment of the substrate and a second one for the fine adjustment close to each grating. The exposed gratings have been developed with OPD 4262, a TMAH (tetra methyl-ammonium-hydroxide) based positive photoresist developer. The resist pattern has been used as a mask for the etching of the chromium layer. For the deep etching of the grating structure into the Fused Silica substrate, RIE processes with Oxygen plasma has been carried out.

The gratings have been characterized in terms of optical performances and structure’s profile. The AFM characterization of grating A (see Fig. 5a) reveals that the profile is close to the desired design. No fabrication artifacts, like misalignment related trenches or walls, affect

#148535 - $15.00 USD Received 2 Jun 2011; revised 8 Jul 2011; accepted 8 Jul 2011; published 15 Jul 2011

the structure. Only a slight roughness is present at the sidewalls. Similarly, a SEM inspection confirms the almost ideal three-level topology. The wavefront measurement of the first diffraction order shows that the phase is uniform overall the grating's area with a rms wavefront–error (WFE) of less than 3 nm.

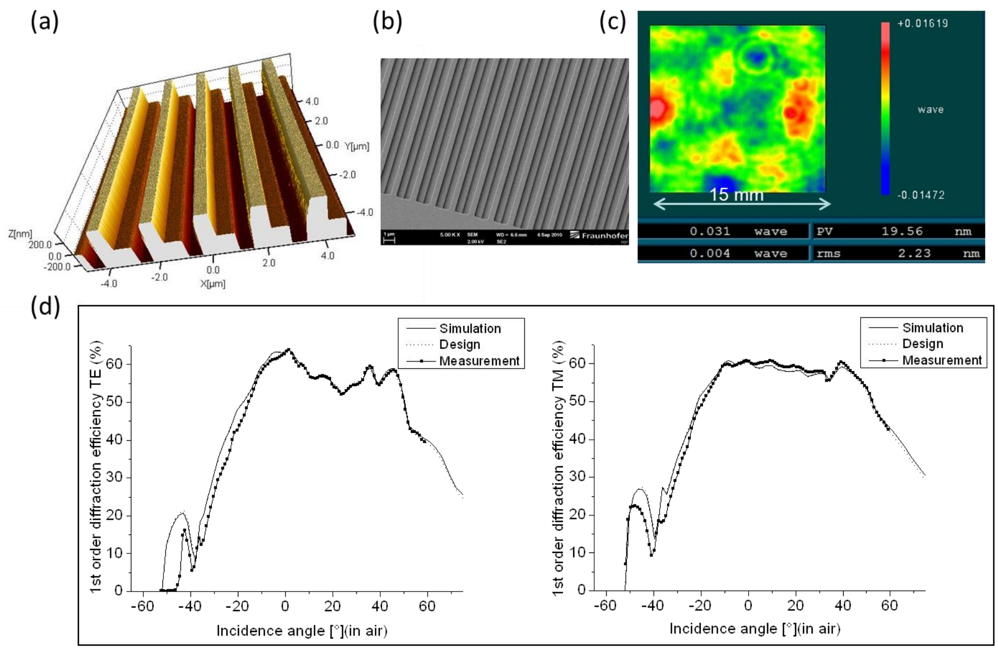

Fig. 5. Characterization of Grating A, (a) AFM 3D measurement. (b) SEM picture of grating A. (c) Interferometric wavefront measurement of the first order diffraction efficiency. (d) First order diffraction efficiency (ratio between first order transmitted intensity and the input intensity inside the substrate) vs. incidence angle: comparison between measured (quadrate-point line) and simulated (original design: dotted line; fabricated grating profile: continuous line) efficiency for TE and TM polarization.

The first order diffraction efficiency vs. incidence angle has been measured for TE and TM polarization. The efficiency of the transmitted first diffraction order has been calculated as power ratio of the relevant transmitted field to the incident laser beam. The Fresnel losses occurring at the back side of the grating's substrate have been considered. The diffraction measurements are in excellent agreement with the rigorous simulations, like shown in Fig. 5d. The efficiency at normal incidence is about 60% as predicted by the design.

The grating B has been characterized in terms of structural profile and diffraction efficiency like done for the grating A. The results are shown in Fig. 6.

AFM measurements (Fig. 6a) reveal the presence of a parasitic structure in comparison to the designed three-level profile. These characterizations suggest a defect depth of about 250 nm and a width of 150 nm. This value of the defect width is strongly overestimated due to the finite dimension of the AFM tip as it is illustrated by the SEM image of the grating (see inset in Fig. 6a). Actual defect widths are typically less than 100nm. According to the used fabrication process, the parasitic structures can be not caused by alignment or sizing problems, but are most probably due to a passivation phenomenon of the side walls during the first RIE etching of level (h_2, w_2) into the substrate. Detailed investigations about the origin of such fabrication defects are still in progress. First results clarify that such parasitic structures are observable after the last deep etching process, as shown in AFM inspections. Their presence is related to the depth of the second etched level, i.e. the larger the depth the more pronounced the artifact. This assertion is justified not only from the comparison with the profile of the grating A, but also from results of other multilevel structures fabricated by different technologies [16]. Because the deep etching is a plasma process, probably during this fabrication step, a protective layer is deposed on the sidewalls. This layer acts like a mask during the remaining etching time. As a consequence, the presence of the layer is related to the final etched depth (see Fig. 6c).

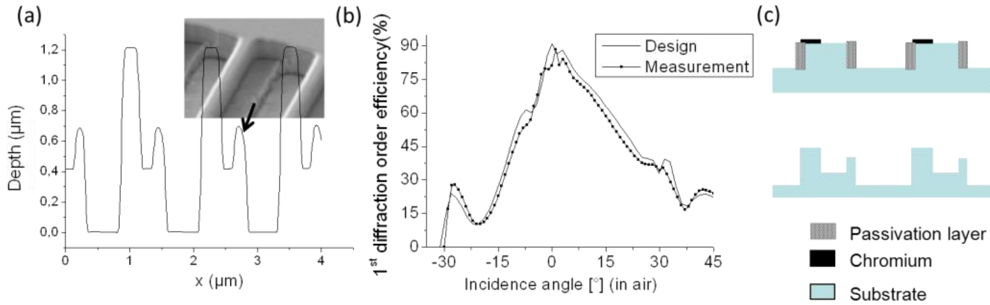

Fig. 6. Characterization of Grating “B”. (a) AFM measurement, inset: section of a corresponding SEM image. (b) First order diffraction efficiency vs. incidence angle: comparison between measured and simulated efficiency for TE polarization. The Simulation is here referred to the original desired profile. (c) Schematic illustration of the formation of the parasitic structure within the etching process.

Despite the presence of these fabrication artifacts, the measured diffraction efficiency in the first order at normal incidence is about 90% as shown in Fig. 6b. Thus, the experimentally obtained efficiency is close to the design value. To understand this astonishing result we simulated the efficiency of the three-level grating including the parasitic structure. Figure 7a shows a mapping of the diffraction efficiency vs. the dimensions (width, depth) of the parasitic artifact.

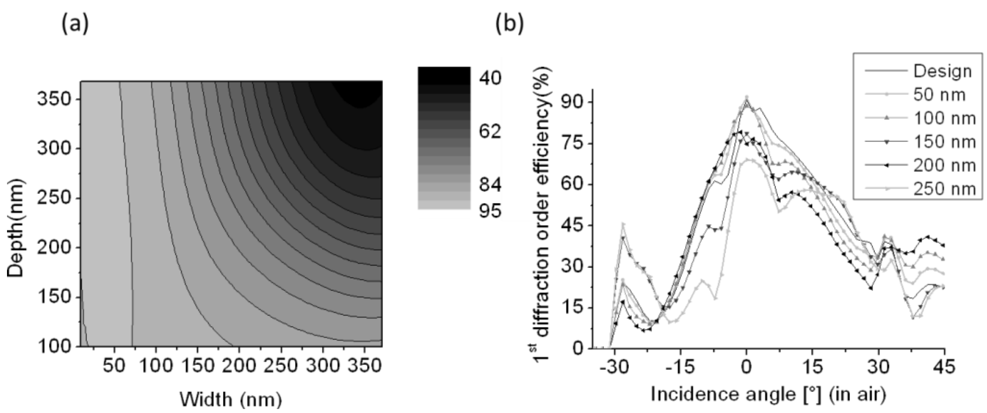

Fig. 7. (a) Influence of the parasitic structures on the efficiency at normal incidence (b) Simulation of diffraction efficiency of grating affected by artifacts of 250 nm depth: influence of the width.

The diffraction efficiency at normal incidence is not significantly reduced by the presence of such parasitic structures of dimensions as measured for grating B. Actually, if the width of the defects is less than approximately 100 nm, the efficiency at normal incidence is almost not influenced. In this case the angular shape of the diffraction efficiency (see Fig. 7b) is nearly unaffected too. Remarkable deviations from the original design occur for larger defect widths.

#148535 - $15.00 USD Received 2 Jun 2011; revised 8 Jul 2011; accepted 8 Jul 2011; published 15 Jul 2011

6. Conclusion

In this work we presented a new technological approach for the fabrication of multilevel gratings in resonance domain to avoid the misalignment errors typical for the classical multistep micro-optics fabrication technology. The new method is based on a single coded chromium mask that contains all information about the critical dimensions of the structures. The realization of this coded mask is the first step of the fabrication process. Then several resist masks are used to select the area of the pattern that will be transferred into the substrate with the desired depth.

The new technological approach has been applied for the fabrication of two different three-level gratings designed in resonance domain. The two gratings differ from period, depth and feature size of the levels according to their different illuminating wavelength and application. The grating's characterization has proven that the *Relaxed Alignment Technology* approach is very suitable for the fabrication of multilevel structures. For one grating with a period to wavelength ratio of about 4.5 and moderate etching depths close to 300 nm the fabrication results are really close to the design leading to e.g. an almost perfect matching between the simulation and the measurement of the diffraction efficiencies for both polarizations.

For the second grating with a period to wavelength ratio of 2 and much larger etching depths, the fabrication generates an artifact: a parasitic structure in the edge of the bottom level, possibly due to a passivation effect in the sidewall, which acts as a mask for the second etching step. This fabrication artifact seems not strictly related to the technological approach, but should be preventable by an appropriate choice of the etching parameters. Nevertheless, further investigations are needed. Despite the presence of this artifact the measured efficiency is about 90%, very close to the design value. This result opens the possibility to design and fabricate new kinds of multilevel gratings by exploitation the process artifacts.

Additionally, the idea to use a resist mask for the different etching steps provides a high flexibility in choosing fabricating of various profiles of the structures which may potentially opens the way towards new diffractive elements in resonance domain.

Acknowledgments

The authors would like to acknowledge the financial support of the Bundesministerium für Bildung und Forschung (BMBF) in the frame of PhoNa project FKZ 03IS2101D and the Deutsche Forschungsgemeinschaft (DFG) within the project SPP1327.

Furthermore, the author would like to thanks the colleagues from the CMN-Optics at Fraunhofer IOF in Jena for their contribution regarding the fabrication of the three-level gratings. A special thanks to Michael Banasch, Tino Benkenstein and André L. Matthes.

The purchase of the e-beam writer SB350 OS at the Fraunhofer IOF has been supported by the European Union (FZK: B 408 – 04004).

#148535 - $15.00 USD Received 2 Jun 2011; revised 8 Jul 2011; accepted 8 Jul 2011; published 15 Jul 2011